Available online at www.sciencedirect.com
ScienceDirect
Earth and Planetary Science Letters 268 (2008) 397–407
EPSL
www.elsevier.com/locate/epsl

4±1.5 °C abrupt warming 11,270 yr ago identified from trapped air in Greenland ice

Takuro Kobashi [a,*], Jeffrey P. Severinghaus [a], Jean-Marc Barnola [b]

[a] *Scripps Institution of Oceanography, University of California, San Diego, La Jolla, CA 92093, USA*
[b] *Laboratoire de Glaciologie et Géophysique de l'Environnement, CNRS, Saint-Martin d'Héres, France*

Received 1 January 2008; received in revised form 20 January 2008; accepted 22 January 2008
Available online 8 February 2008
Editor: M.L. Delaney

Abstract

Nitrogen and argon isotopes in air trapped in a Greenland ice core (GISP2) show two prominent peaks in the interval 11,800–10,800 B.P., which indicate two large abrupt warming events. The first abrupt warming (10±4 °C) is the widely documented event at the end of the Younger Dryas. Here, we report on the second abrupt warming (4±1.5 °C), which occurred at the end of a short lived cooler interval known as the Preboreal Oscillation (11,270±30 B.P.). A rapid snow accumulation increase suggests that the climatic transition may have occurred within a few years. The character of the Preboreal Oscillation and the subsequent abrupt warming is similar to the Dansgaard–Oeschger (D/O) events in the last glacial period, suggestive of a common mechanism, but different from another large climate change at 8,200 B.P., in which cooling was abrupt but subsequent warming was gradual. The large abrupt warming at 11,270 B.P. may be considered to be the final D/O event prior to the arrival of the present stable and warm epoch.

Keywords: Preboreal Oscillation; abrupt climate change; Holocene; Greenland; ice core

1. Introduction

1.1. The Early Holocene and Preboreal Oscillation

After an abrupt warming at the end of the Younger Dryas interval (Severinghaus et al., 1998), Greenland temperature gradually rose by ~5 °C for ~2000 yr and accumulation rate increased by >40% (Cuffey and Clow, 1997). This temperature increase was interrupted by a brief cold event (the Preboreal Oscillation) at 11,400–11,270 B.P. (yr Before Present, where present means C.E. 1950; Fig. 1) (Bjorck et al., 1996, 1997). Abundant evidence of the Preboreal Oscillation has been found in the North Atlantic region from both low and high latitudes, and more evidence is now being found beyond the North Atlantic (Yu and Eicher, 1998; Hu et al., 2006). Bond et al. (1997) found that sea ice was advected toward the south in the North Atlantic during the Preboreal Oscillation (named as Event 8). Atmospheric methane concentration decreased during the Preboreal Oscillation by 8% or 60 ppb (Brook et al., 2000) and the tropical Atlantic had stronger trade winds and lower precipitation (Hughen et al., 1996), suggesting that a broad geographic area experienced this cooling (Brook et al., 2000). Many European pollen studies show that vegetation responded to this cool event (Bjorck et al., 1997). At the time of the Preboreal Oscillation, sea level was still about 50 m lower than present (Bard et al., 1996). A large meltwater pulse (MWP-1B) is inferred to have occurred around this time from an observed rapid sea level rise, potentially causing this brief cool event (Fairbanks, 1989; Bard et al., 1996).

* Corresponding author. Institute for Global Environmental Strategies (IGES), 2108 Kamiyamaguchi, Hayama, Kanagawa, 240-0115 Japan. Tel.: +81 46 855 3871; fax: +81 46 855 3809.
E-mail address: kobashi@iges.or.jp (T. Kobashi).

0012-821X/$ - see front matter © 2008 Elsevier B.V. All rights reserved.
doi:10.1016/j.epsl.2008.01.032

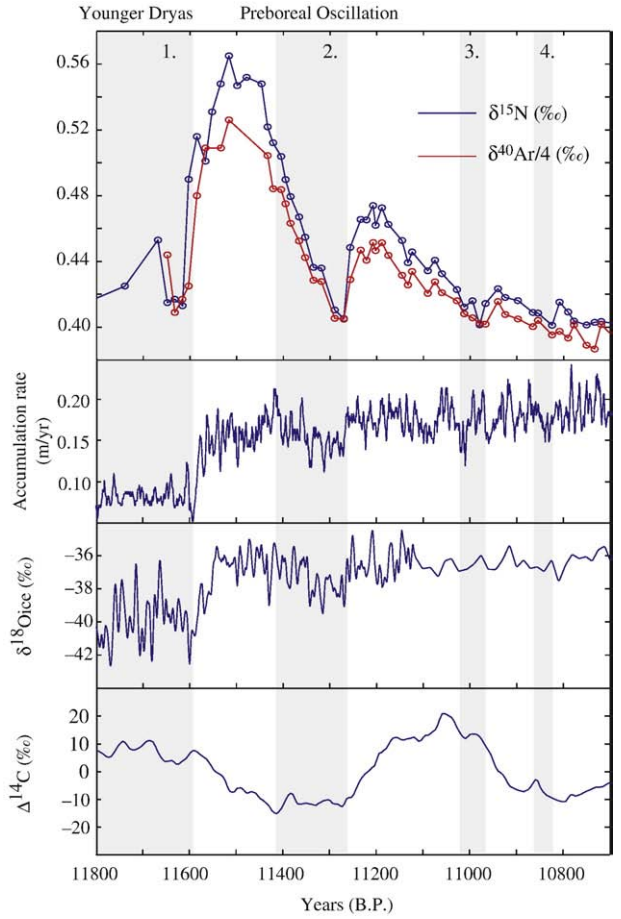

Fig. 1. Measured $\delta^{15}N$ and $\delta^{40}Ar$ in air trapped in ice (GISP2), accumulation rate (Alley et al., 1997b; Cuffey and Clow, 1997), $\delta^{18}O_{ice}$ (Stuiver et al., 1995), and residual $\Delta^{14}C$ from tree rings (Reimer et al., 2004) over the interval 11,800–10,700 B.P. The $\delta^{18}O_{ice}$ and accumulation data were smoothed with a 5-year running mean after a 1-year resolution time series was generated by linear interpolation. $\delta^{15}N$ and $\delta^{40}Ar$ for the period 11,800–11,447 B.P are from Severinghaus et al. (Severinghaus et al., 1998) and for the later part are from Kobashi (2007). The shaded areas numbered as 1 to 4 are cooler periods characterized by $\delta^{15}N$, as follows: (1) the Younger Dryas, (2) the Preboreal Oscillation, (3) the 11.0 ka event, (4) the 10.8 ka event. Note that the resolution of the $\delta^{18}O_{ice}$ record changes after ~11,300 B.P. in the original data (Stuiver et al., 1995).

1.2. Nitrogen and argon isotopes and temperature reconstruction

Over the last decade, isotopic compositions of inert gases in ice cores such as nitrogen and argon have been extensively used to reconstruct past abrupt temperature changes (Severinghaus et al., 1998; Lang et al., 1999; Leuenberger et al., 1999; Severinghaus and Brook, 1999; Landais et al., 2004a,b; Grachev and Severinghaus, 2005; Huber et al., 2006b; Kobashi et al., 2007). Recent advances in measurement techniques have further sharpened the precision of estimates of temperature change (Kobashi, 2007), and a recently completed high resolution Holocene record (10–20 year interval) from GISP2 provides opportunities to understand past climate change during the period when human society went through major changes (Kobashi, 2007; Kobashi et al., 2007).

The basic principles of the method rest on the fact that the isotopic ratios of these gases in the atmosphere are constant for $>10^5$ yr (Mariotti, 1983; Allegre et al., 1987). Therefore, any deviations of isotopic composition in ice cores from atmospheric values are the result of isotopic fractionation in the firn layer (unconsolidated snow on top of glacial ice). The firn layer can be subdivided into three sections in terms of isotopic fractionation (Sowers et al., 1992). The upper few meters of firn is called the "convective zone", in which air freely exchanges with the atmosphere by wind pumping (Colbeck, 1989; Kawamura et al., 2006). Therefore, air in this zone has the same gas composition as the atmosphere (Colbeck, 1989). Below this layer, there is a stagnant layer called the "diffusive air column", where gas is nearly in diffusive equilibrium and transport is dominantly by molecular diffusion (Sowers et al., 1992). Isotopic fractionation occurs in this layer by gravitational settling and thermal diffusion (Severinghaus et al., 1998; Severinghaus and Brook, 1999; Severinghaus et al., 2001). The last layer is called the "non-diffusive zone" or "lock-in-zone", where vertical air movement ceases owing to the existence of impermeable layers of higher-density firn (Sowers et al., 1992). The thickness of the convective zone and non-diffusive zone are likely constant during the Holocene in Greenland, as a model study reproduces gas isotope signals well with an assumption of constant thickness of these two layers (Goujon et al., 2003). Therefore, henceforth we call the thickness of the diffusive air column the "firn thickness".

Gases in the diffusive air column fractionate by at least two mechanisms. First, a change in firn thickness induces a change in gravitational fractionation (Craig et al., 1988; Sowers et al., 1992). Second, a temperature gradient (ΔT) between the top and bottom of the firn induces thermal fractionation (Severinghaus et al., 1998). Measurements of both nitrogen and argon isotopes allow a deconvolution of these two effects, and can be used to infer past firn thickness and ΔT (Severinghaus and Brook, 1999; Landais et al., 2004a,b). The method is most effective for investigating decade-scale abrupt climate changes, which create a large ΔT and thus large isotopic signals (Severinghaus and Brook, 1999; Landais et al., 2004a,b). The method is not very effective on multi-centennial scales, because the firn thermally equilibrates on these timescales (Allegre et al., 1987).

The surface temperature reconstruction from ΔT is not straightforward for higher (>0.05 yr^{-1}) or lower (<0.005 yr^{-1}) frequencies because there is no single unique solution, due to smoothing of the record by gas diffusion and bubble close-off, and due to thermal equilibration. As various surface temperature histories can satisfy the observed gas-isotopic signals, oxygen isotope records of ice ($\delta^{18}O_{ice}$) have been used by some studies to provide constraints on the "shape" and rate of surface temperature change, thus reducing the dimensionality of the problem (Landais et al., 2004a; Huber et al., 2006b; Kobashi et al., 2007). However, $\delta^{18}O_{ice}$ is not only a proxy of temperature. It may vary without temperature change, or it may be biased by other climatic variables such as the evaporative origins of the moisture, or changes in the seasonality of precipitation (Charles et al., 1994; Jouzel et al., 1997; White et al., 1997). For these reasons, direct methods of temperature

reconstruction without $\delta^{18}O_{ice}$ have been explored (Landais et al., 2004b). In this study, we developed a new method to reconstruct a surface temperature history without using $\delta^{18}O_{ice}$, based on simultaneous measurements of nitrogen and argon isotopes.

2. Methodology

2.1. Chronology

A precise chronology is critical to compare climate information in ice cores with other paleoclimatic archives, for example those dated by ^{14}C. Recent advances in the tree-ring chronology provide an absolutely dated tree-ring chronology back to 12,410 B.P. (Friedrich et al., 2004). Therefore, it is now possible to correlate regional climate changes with unprecedented accuracy for the early Holocene (Friedrich et al., 2004; Reimer et al., 2004).

We used an ice core (GISP2) from central Greenland (72° 36′N 38° 30′W; 3203 m asl), with a layer-counted time scale from visual stratigraphy (Alley et al., 1997b; Cuffey and Clow, 1997). This chronology may be too old in the early to middle Holocene by ~100 yr, as inferred from a correlation between ^{10}Be in the ice cores and ^{14}C from tree-rings (Finkel and Nishiizumi, 1997; Kobashi et al., 2007). Therefore, it requires some adjustment. A recent Greenland ice core chronology (GICC05) for GRIP, NGRIP, and DYE-3 places the termination of the Younger Dryas at 11,653 B.P. (Vinther et al., 2006). However, the correlation of ^{10}Be from the ice core and ^{14}C from tree-rings shows that this chronology is ~80 yr too old in the early Holocene (R. Muscheler, personal communication), which suggests that the age of the Younger Dryas termination should be ~11,573 B.P. As another piece of evidence for the age of the Younger Dryas termination, the German tree ring chronology exhibits a rapid increase in tree ring width at 11,590 B.P (Friedrich et al., 1999, 2004). As the uncertainty of dendrochronology is estimated to be less than 1 yr for this interval (M. Friedrich, personal communication), the year 11,590 B.P. should be the best estimate for the age of the Younger Dryas termination. The GISP2 visual stratigraphy timescale has the age of the Younger Dryas termination at 11,705 B.P inferred from the rapid increase of accumulation rate (Alley et al., 1997b; Cuffey and Clow, 1997). Therefore, we subtracted 115 yr from the GISP2 chronology to align it with the tree-ring age of the Younger Dryas termination. See the electronic Appendix A for the data of this chronology.

We used a firn densification-heat transfer model (Goujon et al., 2003) to estimate a preliminary gas age from input temperature and accumulation rate. These inputs were obtained from the borehole-calibrated $\delta^{18}O_{ice}$ and ice-flow corrected layer thickness records of Cuffey and Clow (1997) (Cuffey and Clow, 1997). The calculated gas-ice age difference (~450 yr around 12,270 B.P.) is estimated to have an uncertainty of 10% or ±45 yr (Goujon et al., 2003). We find a rapid increase in accumulation rate, and oxygen isotope ratio of ice, at 11,270 B.P. (Fig. 1), which should correspond to the rapid increase observed in ΔT at 11,245 B.P. in the preliminary gas age. Therefore, we added 25 yr to the calculated gas age to align the gas signal with the ice signal of the warming (Fig. 1). Relative ice-age uncertainty at century scales in the early Holocene is estimated to be ~1% (Alley et al., 1997b). Therefore, the age difference of 320 yr between the termination of the Younger Dryas and the abrupt warming at 11,270 B.P. yields ~4 yr relative uncertainty. Although it is difficult to identify all the uncertainties, we estimate the absolute uncertainty of reported calendar ages herein to be ±30 yr from the above information.

2.2. Inert gas isotopes and isotopic fractionation in the firn layer

We analyzed argon (mass 40 and 36) and nitrogen (mass 15 and 14) isotope ratios ($\delta^{15}N$ and $\delta^{40}Ar$) in air trapped in the GISP2 ice core (Fig. 1) (Kobashi, 2007). Data before 11,446 B.P. are from Severinghaus et al. (1998), and data in the later part is from Kobashi (2007) and presented in the electronic Appendix A. The two datasets for $\delta^{15}N$ show good agreement for the overlapping four points (Fig. 2). From 11,466 B.P. to 10,000 B.P. the data resolution is about 20 yr, and each data point is from a single sample (Kobashi, 2007). We only use data from Kobashi (2007) for surface temperature calculation because of its continuity and precision. The isotopic ratios are presented as a deviation from the present atmospheric composition (which is the standard) by conventional notation as follows.

$$\delta^{40}Ar = \left(\left(^{40}Ar/^{36}Ar_{sample}\right)/\left(^{40}Ar/^{36}Ar_{standard}\right) - 1\right)*10^3‰ \quad (1)$$

$$\delta^{15}N = \left(\left(^{15}N/^{14}N_{sample}\right)/\left(^{15}N/^{14}N_{standard}\right) - 1\right)*10^3‰ \quad (2)$$

Significant analytical improvements have been made since the first publication of this kind of data for the Younger Dryas (Severinghaus et al., 1998). Improved precisions of $\delta^{15}N$ and $\delta^{40}Ar$ for this study are estimated to be 0.004‰ and 0.016‰, respectively. The analytical method is described elsewhere (Kobashi, 2007). Each observed $\delta^{15}N$ and $\delta^{40}Ar$ value can be decomposed into two components as discussed previously.

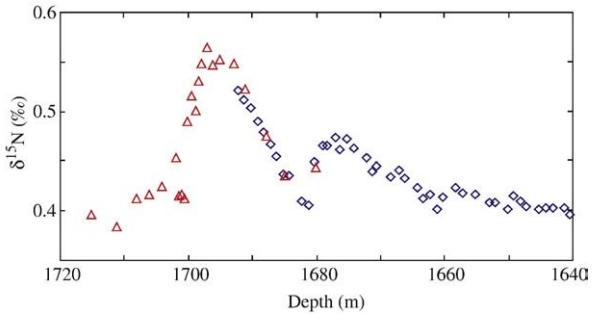

Fig. 2. $\delta^{15}N$ records in the depth interval 1720 m to 1640 m. The triangles are means of replicate data from Severinghaus et al. (1998) (Severinghaus et al., 1998), and the diamonds are from Kobashi (2007).

Therefore, the observed $\delta^{15}N$ ($\delta^{15}N_{obs}$) and $\delta^{40}Ar$ ($\delta^{40}Ar_{obs}$) may be written as

$$\delta^{15}N_{obs} = \delta^{15}N_{grav} + \delta^{15}N_{therm}{}^{15}\gamma = \delta^{15}N_{grav} + \Delta T^{15}\Omega^{15}\gamma \quad (3)$$

$$\delta^{40}Ar_{obs} = \delta^{40}Ar_{grav} + \delta^{40}Ar_{therm}{}^{40}\gamma = \delta^{40}Ar_{grav} + \Delta T^{40}\Omega^{40}\gamma \quad (4)$$

$$^{15}\gamma \cong {}^{40}\gamma \quad (5)$$

where the subscripts 'therm' and 'grav' represent thermal and gravitational components, respectively, $^{15}\gamma$ is a disequilibrium term, and $^{15}\Omega$ is the thermal diffusion sensitivity of $\delta^{15}N$ (Grachev and Severinghaus, 2003b). The disequilibrium terms are negligible for timescales longer than the firn diffusion time of ~10 yr (Schwander et al., 1993), and are ignored in this study ($^{15}\gamma = 1$). The gravitational component depends on the absolute mass difference, which is 4.007 times larger for $\delta^{40}Ar$ than for $\delta^{15}N$ (Craig et al., 1988). Therefore, we can express it as $\delta^{15}N_{grav} \cong \delta^{40}Ar_{grav}/4$.

$$\delta^{40}Ar_{obs} = \delta^{15}N_{grav} \times 4 + \Delta T^{40}\Omega^{15}\gamma \quad (6)$$

For simplicity, we use $\delta^{40}Ar/4$ rather than $\delta^{40}Ar$ in the following discussion so that the gravitational signals for nitrogen and argon isotopes are on the same scale. The past firn temperature gradient ΔT can be calculated from the difference ($\delta^{15}N_{excess} = \delta^{15}N_{obs} - \delta^{40}Ar_{obs}/4$), which is sensitive to the differing thermal responses of $\delta^{15}N$ and $\delta^{40}Ar/4$. It is noted that the precision of $\delta^{15}N_{excess}$ is significantly improved from the previous studies as argon and nitrogen isotopes were measured simultaneously for this period (Kobashi, 2007). Grachev and Severinghaus (2003a,b) conducted laboratory experiments to obtain the thermal coefficients of $\delta^{15}N$ and $\delta^{40}Ar$ in air, which are a prerequisite for precise estimates of temperature changes. With these numbers, ΔT (°C) can be calculated simply as ΔT (°C) = $\delta^{15}N_{excess}$(‰)/0.0047 ± 0.0005 (‰/°C) (Severinghaus and Brook, 1999; Grachev and Severinghaus, 2003a,b).

$$\left(\delta^{15}N_{obs} - \delta^{40}Ar/4_{obs}\right) = \Delta T^{15}\gamma\left({}^{15}\Omega - {}^{40}\Omega/4\right) \equiv \delta^{15}N_{excess} \quad (7)$$

$$^{15}\Omega - {}^{40}\Omega/4 = 0.0047 \pm 0.0005‰°C^{-1} \quad (8)$$

The gravitational component can be calculated as a residual of observed $\delta^{15}N$ corrected for the thermal component (Severinghaus et al., 2003). So, $\delta^{15}N_{grav} = \delta^{15}N - {}^{15}\Omega * \Delta T$ where $^{15}\Omega = 0.0145 \pm 0.0004$‰/°C at 240 K, the thermal diffusion sensitivity of $\delta^{15}N$ (Grachev and Severinghaus, 2003b). Note that the thermal coefficients are temperature dependent, but in the temperature range of −34 °C to −42 °C their difference is nearly constant within analytical uncertainty (Grachev and Severinghaus, 2003a,b). Diffusive column height (DCH) or firn thickness can be calculated from $\delta^{15}N_{grav}$ (Schwander et al., 1997; Severinghaus et al., 2003).

$$DCH(m) = RT/(g\Delta m)\left(\ln\left(\delta^{15}N_{grav}/1000 + 1\right)\right) \quad (9)$$

where R is the ideal gas constant (8.314 J mol^{-1} K^{-1}), T is temperature (K), g is the acceleration due to gravity (9.82 m s^{-2}), and Δm is the mass difference between ^{15}N and ^{14}N (0.001 kg mol^{-1}).

2.3. Gas loss and normalization problems

Recent studies show that gas composition in ice cores may change during/after the coring process (Bender et al., 1995; Severinghaus et al., 2003; Kobashi, 2007). At least two mechanisms may affect gas composition (Kobashi, 2007). First, smaller molecules with less than a certain threshold size (~3.6) leak out of the ice lattice with little isotopic fractionation, as observed in firn air and ice core studies (Bender et al., 1995; Huber et al., 2006a; Severinghaus and Battle, 2006; Kobashi, 2007). This mechanism appears nearly independent of mass. Second, gases in ice leak through microcracks causing mass-dependent fractionation, which is often observed in poor quality ice and the gas–clathrate transition zone where ice samples are typically fractured (Bender et al., 1995; Kobashi, 2007). The mixture of these two processes complicates interpretation. As the GISP2 ice core at the depth of our study is of good quality and is out of the gas–clathrate transition (Kobashi, 2007), gas loss impacts on isotopes can be considered to be relatively small.

A recent study (Kobashi, 2007) applied the same method (isotopic measurements and ΔT calculation) to the last 1000 yr, and found that argon isotopes in this depth range in the core are likely affected by gas-loss. The study also found that $\delta Ar/N_2$ is a good proxy indicator for the amount of argon isotopic fractionation by gas loss, as previously reported by (Severinghaus et al., 2003). The magnitude of argon isotopic fractionation was found to be −0.0075‰ per ‰ in $\delta Ar/N_{2\text{-corrected}}$ (Kobashi, 2007).

Prior work has found that both $\delta^{15}N$ and $\delta^{40}Ar/4$ may shift slightly and systematically on the order of 0.005–0.010‰ owing to analytical problems during the normalization of data to present atmosphere, the standard used (Severinghaus and Brook, 1999; Grachev, 2004; Kobashi, 2007). This slight shift creates a constant offset in the ΔT estimates, and significantly affects the surface temperature calculation as described below. Without any further information, the normalization problems are difficult to constrain. As we discuss later, we attempt to calibrate for the normalization problem by matching model results with observed isotope records.

2.4. Surface temperature calculation — a new method

Since the original study of Severinghaus et al. (1998), there have been many attempts to quantify surface temperature changes with gas isotope records (Lang et al., 1999; Leuenberger et al., 1999; Severinghaus and Brook, 1999; Landais et al.,

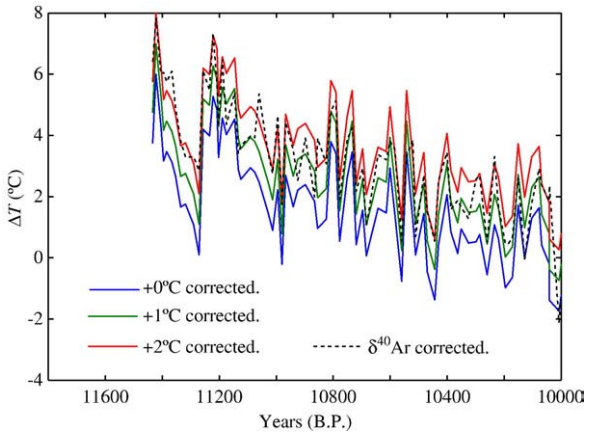

Fig. 3. Firn temperature gradient (ΔT) records from 11,800 B.P. to 10,000 B.P. The observed ΔT records after 11,417 B.P. are used as inputs for four experiments. The blue line is ΔT shifted by 0.0 °C, the green line is ΔT shifted by 1.0 °C, the red line is ΔT shifted by 2.0 °C, and the dotted line is ΔT with δ^{40}Ar corrected. (For interpretation of the references to colour in this figure legend, the reader is referred to the web version of this article.)

2004a,b; Grachev and Severinghaus, 2005; Huber et al., 2006b). To reconstruct surface temperature changes, it is necessary to understand changes in the firn condition due to heat diffusion and advection, densification, and the bubble close-off process. The firn condition and associated change can be explicitly calculated from empirical glaciological models if surface temperature and accumulation rate histories are known (Schwander et al., 1997; Goujon et al., 2003). By combining gas-isotope data with firn-densification models, various methods have been developed to reconstruct surface temperature changes. A few studies used prescribed shapes of temperature histories, such as a step function, to estimate magnitudes of temperature changes (Severinghaus et al., 1998; Severinghaus and Brook, 1999) Others reconstructed the surface temperature change by calibrating $\delta^{18}O_{ice}$ (Lang et al., 1999; Leuenberger et al., 1999; Landais et al., 2004a; Huber et al., 2006b; Kobashi et al., 2007). Landais et al. (2004b) explored a full range of the potential magnitude of temperature change from isotope records.

A rapid surface temperature change, if it is instantaneous or much faster than heat diffusion in firn, equals the temperature gradient (ΔT) in the firn layer (assuming an isothermal initial state). If it happens gradually (over a few decades or longer), the temperature gradient (ΔT) in firn progressively becomes smaller than the surface temperature change owing to heat transfer in the firn. To calculate surface temperature the heat transfer in firn needs to be considered, which is also a function of ΔT. In light of these circumstances, we modified the firn densification-heat transfer model (Goujon et al., 2003) to calculate surface temperature from the ΔT history and accumulation rate. We used an accumulation rate history obtained from visual layer counting (Alley et al., 1997b) coupled with ice-flow correction from a glaciological model (Cuffey and Clow, 1997).

After the modification, the model calculation proceeds as follows. In a model year, a new firn state is forced by a new surface temperature and accumulation rate. With the new forcing from the surface, heat diffusion/advection and firn densification is calculated. In the next model year, a new surface temperature (T_s) is obtained by adding the calculated temperature (T_b) at the bottom of firn in the previous model-year to ΔT obtained from observed δ^{15}N and δ^{40}Ar.

$$T_s = T_b(\text{model output from the previous model year}) + \Delta T(\text{observation})$$

By repeating this process, the surface temperature history can be calculated recursively. To initialize, the model uses calibrated $\delta^{18}O_{ice}$ as surface temperature (Cuffey and Clow, 1997) until 11,417 B.P., and from that point on it switches to the method described above. Annual-resolution ΔT data are obtained by linearly interpolating the original data (~20-year resolution).

One modification from the original Goujon model (Goujon et al., 2003) is made to the calculation of isotopic fractionation. The firn condition is calculated with two different coordinate systems in the model (Goujon et al., 2003). A Lagrangian coordinate system is used to calculate the temperature field in the firn, and an Eulerian coordinate system is used for the calculation of the age of the gas. We found that the results from the two coordinate systems disagree slightly, with the changes in firn thickness in the Eulerian coordinate system showing a slight lag to those in the Lagrangian coordinate system. To be consistent between the temperature field and firn thickness, we modified the original code to use the Eulerian coordinate for the calculation of gravitational fractionation, which is a function of firn thickness.

One drawback of this new method is that small errors in ΔT are cumulative, as in a random walk, such that surface temperature error grows with time. For this reason, calibration against independent data sets is necessary, such as borehole temperatures or gas-based firn thickness data (see below).

3. Results

3.1. Isotope Data

The isotope records show two prominent peaks in the interval 11,800 B.P. to 10,700 B.P. (Fig. 1). The combined analysis of nitrogen and argon isotopes suggests that two large abrupt warming events occurred during this period. The first warming occurred at 11,590 B.P., marking the end of the Younger Dryas (Alley et al., 1993; Severinghaus et al., 1998). The second one occurred at 11,270 B.P. at the end of the Preboreal Oscillation. Rather abrupt changes are also evident in the $\delta^{18}O_{ice}$ and snow accumulation rate (Fig. 1). The magnitudes of the two peaks in δ^{15}N and δ^{40}Ar/4 are 0.14‰ and 0.11‰ for the Younger Dryas termination, and 0.06‰ and 0.04‰ for the termination of the Preboreal Oscillation, respectively. The ratios $(\Delta\delta^{40}\text{Ar}/4)/\Delta\delta^{15}\text{N}$ of these changes are 0.78 for the Younger Dryas and 0.67 for the Preboreal Oscillation. As the ratio $(\Delta\delta^{40}\text{Ar}/4)/\Delta\delta^{15}\text{N}$ of thermal responses of δ^{15}N and δ^{40}Ar to a temperature change is 0.68 (Grachev and Severinghaus, 2003a,b), it can be inferred that the peak at the terminal Younger Dryas event consists of ~85% thermal and ~15% gravitational signals. The peak at the

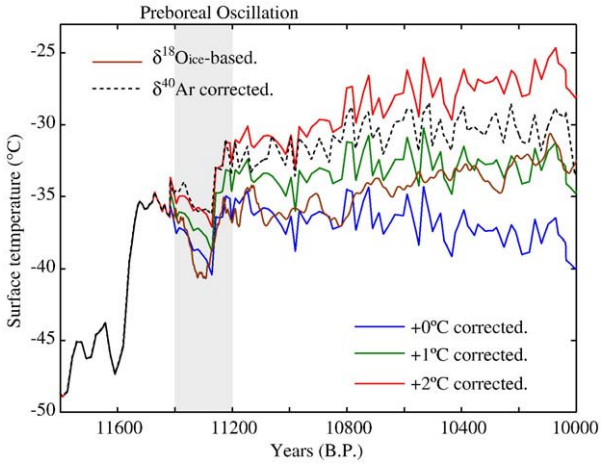

Fig. 4. Surface temperature reconstructions with the ΔT-based and $\delta^{18}O_{ice}$-based methods. The blue, green, red, and dotted lines are the surface temperature reconstructions with ΔT shifted by +0.0 °C, +1.0 °C, +2.0 °C, and corrected δ^{40}Ar, respectively. The black and brown lines are the $\delta^{18}O_{ice}$-based surface temperature reconstruction (Cuffey and Clow, 1997). The shaded area shows the two centuries (11,400–11,200 B.P.) spanning the Preboreal Oscillation and the subsequent abrupt warming. (For interpretation of the references to colour in this figure legend, the reader is referred to this article.)

end of the Preboreal Oscillation nearly all comes from a thermal signal. The ΔT shows an abrupt increase of 4.1 °C at 11,271 B.P. (Fig. 3), which is about half of the observed ΔT (8 °C) at the Younger Dryas termination (Grachev and Severinghaus, 2005). δ^{15}N shows two other smaller oscillations around 10,940 B.P. and 10,800 B.P. with amplitudes of ~0.02‰ and 0.015‰, respectively (numbered as 3 and 4 in Fig. 1), which are also interpreted here as small abrupt warming events. The durations of one cycle decrease progressively from ~320, to ~290, to ~150, and to ~50 yr, an interesting fact that will be discussed below.

3.2. Surface temperature reconstruction

3.2.1. 11,417 B.P. to 10,000 B.P.

As mentioned in the data description, our approach to surface temperature reconstruction using ΔT requires an adequate calibration, due to possible artifacts. Therefore, we conducted four model experiments to find the best fit between model and observed data (δ^{15}N and firn thickness) by adjusting a correction to ΔT. The temperature calculation depends on an initial temperature profile of the firn and ice sheet, especially for the first few hundred years of the integration. We assume that a temperature history before 11,417 B.P. can be reconstructed from the calibrated $\delta^{18}O_{ice}$ with the borehole temperature (Cuffey and Clow, 1997), and we force the model with this temperature until 11,417 B.P. Although a $\delta^{18}O_{ice}$-based surface temperature with a single calibration equation is clearly problematic (Landais et al., 2004a; Huber et al., 2006b) owing to the variable oxygen-temperature coefficient with time (Cuffey et al., 1997), a model driven with the δ^{18}O-based surface temperature reproduces δ^{15}N and δ^{40}Ar sufficiently well (Goujon et al., 2003; Kobashi, 2007). Therefore, the use of the calibrated $\delta^{18}O_{ice}$ should be valid in the first order and as a starting point for our method (Goujon et al., 2003; Kobashi, 2007).

The model experiments are conducted with three ΔT time series corrected by +0.0 °C, +1.0 °C, and +2.0 °C for the possible standardization problems, and a ΔT time series from corrected argon isotopes using $\delta Ar/N_2$ to address potential gas-loss problems (Fig. 3). The shifts are accommodated into the isotopic values by subtracting a constant value of 0.0047 (‰/°C) ×0.0 °C, ×1.0 °C, and ×2.0 °C from δ^{40}Ar/4, respectively [the value of 0.0047 (‰/°C) is the sensitivity of $\delta^{15}N_{excess}$ to a 1 °C temperature gradient (Grachev and Severinghaus, 2003a,b)]. The argon isotope correction is made following the method of (Severinghaus et al., 2003) with a coefficient of −0.0075‰ per 1‰ change in gravitationally and thermally corrected $\delta Ar/N_2$ (Kobashi, 2007).

Model results of the four ΔT-based surface temperature reconstructions, along with the $\delta^{18}O_{ice}$-based temperature reconstruction, provide a means to assess the possible artifacts (Fig. 4). The reconstruction with no ΔT shift (blue) shows a gradual cooling after the Preboreal Oscillation, whereas the scenario with +1 °C shift (green) shows a modest temperature increase after the Preboreal Oscillation. The reconstruction with +2 °C shift (red) shows a large temperature increase after the Preboreal Oscillation, reaching almost −25 °C at 10,000 B.P. The reconstruction with $\delta^{40}Ar_{corrected}$ shows a gradual warming until 10,600 B.P. The $\delta^{18}O_{ice}$-based reconstruction (brown) shows a temperature history similar to the 0 °C-shift until 10,800 B.P., when it starts to fit better with the ΔT +1 °C scenario (Fig. 4).

An additional constraint is available from the fit of the model to observed δ^{15}N (Fig. 5). The overall gradual decrease of δ^{15}N after ~11,500 B.P. reflects decreasing firn thickness and firn temperature gradient as the firn adjusts to Holocene warmth. The ΔT +1 °C scenario (green) shows the closest agreement with the observed δ^{15}N. Somewhat surprisingly, the reconstruction with $\delta^{40}Ar_{corrected}$ shows less agreement with observation, in contrast to the result for the last 1000 yr (Kobashi, 2007).

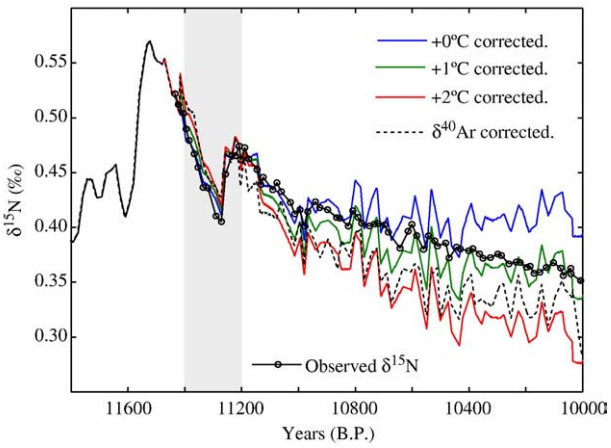

Fig. 5. Modeled and observed δ^{15}N. The blue, green, and red lines are the modeled δ^{15}N with ΔT shifted by +0.0 °C, +1.0 °C, +2.0 °C, and corrected δ^{40}Ar, respectively. The circles are the observed δ^{15}N. The black line before 11,417 B.P. is the model result with the $\delta^{18}O_{ice}$-based surface temperature. The shaded area is as in Fig. 4. (For interpretation of the references to colour in this figure legend, the reader is referred to the web version of this article.)

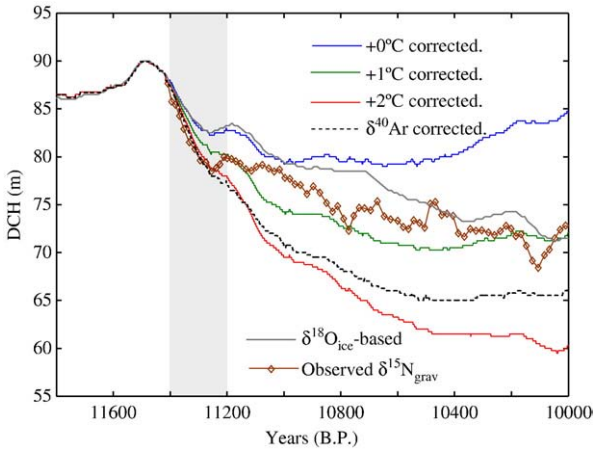

Fig. 6. Observed and modeled diffusive column height (DCH or firn thickness) from 11,800 B.P. to 10,000 B.P. The lines before 11,417 B.P. are model results with the $\delta^{18}O_{ice}$-based surface temperature. The blue, green, red, and dotted lines are the modeled DCH with ΔT shifted by +0.0 °C, +1.0 °C, +2.0 °C, and corrected $\delta^{40}Ar$, respectively. The diamonds are the DCHs computed from the observed $\delta^{15}N_{grav}$ computed from ΔT (+1.0 °C correction). Note that the data are smoothed by a 5-point running mean (covering about 100 yr for each point). The grey line is the model result with the $\delta^{18}O_{ice}$-based surface temperature. The shaded area is as in Fig. 4. (For interpretation of the references to colour in this figure legend, the reader is referred to the web version of this article.)

This may suggest that argon isotopic fractionation associated with gas loss in the clathrate zone may have a different fractionation coefficient than in the shallow bubbly ice zone. The variation of $\delta Ar/N_2$ is larger in this zone than in shallower depths (0–1000 m) (Kobashi, 2007), suggesting that gas and clathrate may be coexisting in this depth interval making the $\delta^{40}Ar$ gas-loss correction difficult. The modeled $\delta^{15}N$ in general shows more fluctuation than the measurements, partly owing to the poorer relative precision of ΔT.

A further constraint is provided by the fit of DCH (or firn thickness) to the observed DCH, which is calculated from $\delta^{15}N_{grav}$ (smoothed with a 5-point running mean). At 11,600–11,400 B.P., the modeled DCH shows the highest value of ~90 m in this interval. Then, it rapidly decreases in response to the enhanced densification caused by the abrupt warming at the Younger Dryas termination. The DCH turns upwards around 11,250 B.P. in response to the cooling during the Preboreal Oscillation, and then the DCH starts decreasing around 11,210 B.P owing to the surface warming at 11,270–11,250 B.P. The time lag is found to be ~100 yr between the changes in surface temperature and DCH, owing to the slow heat transfer in the firn. The model results seem to correctly reconstruct the time lag for the Preboreal Oscillation, although later fluctuations in the observed DCH are not reproduced well by the model results. The DCH reconstruction with ΔT shifted by +1 °C (green) again shows the closest agreement with observation (Fig. 6).

Recent studies (Zwally and Jun, 2002; Li et al., 2003) found that interannual variation of firn thickness was 40–80 cm during the period of 1992–1999 with seasonal variation of nearly 1 m in central Greenland, due to changes in temperature and accumulation. These magnitudes are much larger than expected from conventional firn densification models (Zwally and Jun, 2002). This discrepancy is likely due to a higher dependence of the firnification process on temperature than accounted for by conventional models (Zwally and Jun, 2002). The low centennial fluctuations in our model DCH may suggest that the shallow firn densification parameterization in the Goujon model (Goujon et al., 2003) may need to be revised.

Temperature signals in gas isotope data are opposite in $\delta^{15}N_{grav}$ and $\delta^{15}N_{therm}$, because a surface warming creates a positive $\delta^{15}N_{thern}$ signal, and a negative $\delta^{15}N_{grav}$ signal due to thinning firn. Therefore, small surface temperature fluctuations, generating near-simultaneous changes in the shallow firn thickness and temperature gradient, can be canceled in the observed $\delta^{15}N$. To reconstruct observed isotope signals, it is important to have a realistic model representation of shallow firn densification processes, which are currently poorly understood.

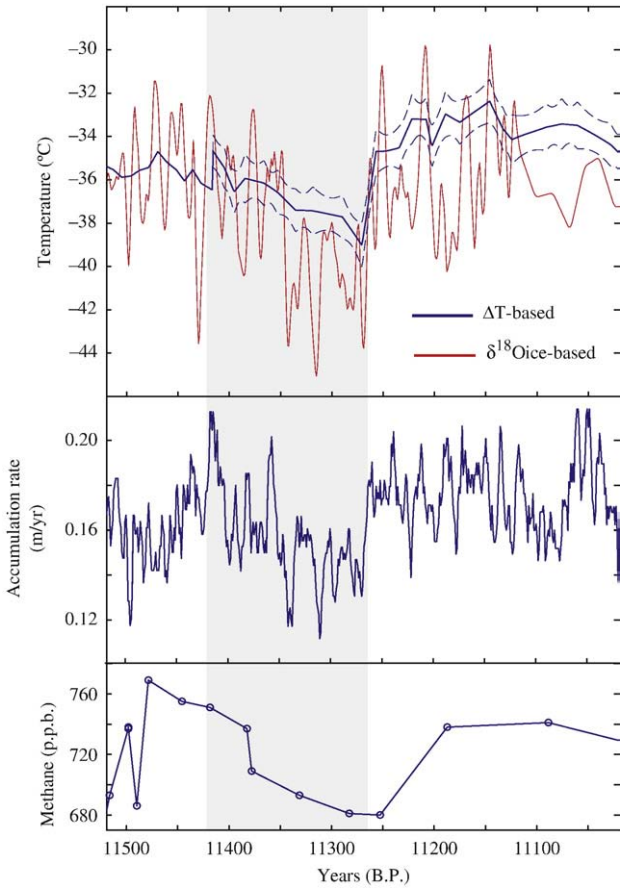

Fig. 7. Reconstructed surface temperature records (this study), accumulation rate (Alley et al., 1997b; Cuffey and Clow, 1997), and atmospheric CH_4 concentration (Brook et al., 2000) from GISP2 ice. (Top) The thick blue line is the ΔT-based surface temperature reconstruction with the +1 °C shift, and the dashed blue lines are 1σ errors. The red line is the $\delta^{18}O_{ice}$-based surface temperature reconstruction (Cuffey and Clow, 1997). The accumulation rate and the $\delta^{18}O_{ice}$-based temperature are smoothed with a 5-year running mean as for Fig. 1. The shaded area includes the Preboreal Oscillation and subsequent abrupt warming at 11,270 B.P. To estimate 1σ error, 100 realizations of synthetic ΔT records were generated by Monte Carlo simulation by adding white noise to the ΔT data with a standard deviation of 1 °C, which was obtained from the error estimate (0.8 °C) for the last millennium dataset plus 20% (Kobashi, 2007). Then, the 100 realizations of surface temperatures were used to calculate mean surface temperature and the error (1σ).

3.3. Preboreal Oscillation and abrupt warming at 11,270B.P.

The reconstructed surface temperature with the ΔT-based method shows a gradual cooling after the abrupt warming at the Younger Dryas termination, and then abruptly warms by 4± 1.5 °C (decadal average) at the end of the Preboreal Oscillation (11,271±30 yr B.P.; Figs. 1 and 7). We found that chronological uncertainty (mainly from the gas-ice age difference) has little effect on this estimate (<0.1 °C). The ΔT time series shows that the temperatures increased by 4.1 °C for all three scenarios of constant ΔT shift, and 3.3 °C for $\delta^{40}Ar_{corrected}$. The change occurs in only one sample interval between 11,271 B.P. (1681.21 m) and 11,257 B.P. (1680.32 m). Considering that gas diffusion and bubble close-off processes smooth isotopic signals, this warming very likely occurred in less time than the sample interval of 14 yr. The fact that accumulation rate increased by 30% in a few years (Fig. 7) suggests the climate reorganization was very rapid, similar to the Younger Dryas termination (Alley et al., 1993). The results of the three model experiments produce nearly the same temperature change of 4 °C because of its rapidity, which confirms the robustness of the temperature estimate.

In the case of abrupt warming after stable climate, the change in ΔT is typically smaller than the surface temperature change owing to temperature diffusion. In this study, however, the model produces a slightly smaller surface temperature change (<0.1 °C) than the observed ΔT change. The most pronounced contrast was found in the scenario with a zero ΔT-shift, but a 1 °C ΔT-shift also showed this effect. This can be explained by the fact that the cold wave from the cooling during the Preboreal Oscillation continued to diffuse deeper during the surface warming (temperature inversion in Fig. 8). This points to the fact that an estimation of abrupt temperature changes from a ΔT record requires understanding of the preceding temperature trend.

Cuffey et al. (Cuffey et al., 1995; Cuffey and Clow, 1997) reconstructed past temperature by calibrating $\delta^{18}O_{ice}$ with borehole temperature. They found a calibration of T (°C)= [$\delta^{18}O_{ice}$ (‰)+24.72]/0.328 for times older than 8,000B.P.

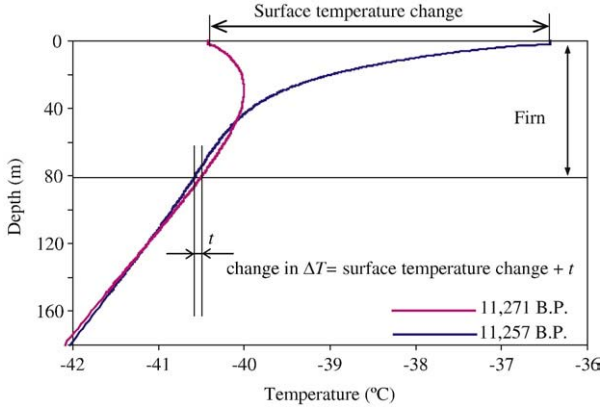

Fig. 8. Model outputs of the temperature profile of the firn and ice sheet before and after the abrupt warming at 11,270 B.P in the ΔT-based surface temperature reconstruction (0.0 °C -shift). Firn depth is estimated to be ~82 m from the model.

The $\delta^{18}O_{ice}$-based surface temperature (Cuffey and Clow, 1997) shows a rapid temperature decrease at 11,350 B.P, with sustained cold for ~80 yr (Fig. 7). This trend creates a symmetrical shape (rapid cooling and warming) in the decadal climate change, which is different from our ΔT-based surface temperature history. The ΔT-based temperature record shows that the temperature after the Preboreal Oscillation was warmer than prior to the event (Figs. 4 and 7). This may be consistent with observations of a two step warming from the Younger Dryas to the Preboreal, as some European paleoclimate evidence suggests (Seppa et al., 2002).

4. Discussion

4.1. Atmospheric methane concentration

Atmospheric methane concentration can be considered as a crude hemispheric climate integrator because of its relatively long lifetime of 8 yr (compared to the atmospheric mixing time of ~1 yr) (Brook et al., 2000; Kobashi et al., 2007). Methane concentration reached 769 ppb at 11,479 B.P. (Brook et al., 2000). Then, it gradually decreased toward a minimum at 11,253 B.P. owing to cooler and/or drier climate, and rose by 58 ppb in one data interval at the end of the Preboreal Oscillation (Fig. 7). The character of methane change during the Preboreal Oscillation is more similar to the ΔT-based surface temperature than the $\delta^{18}O_{ice}$-based temperature (Fig. 7). The lowest methane concentration of 680 ppb during the Preboreal Oscillation occurs at 11,253 B.P or 1680.12 m in the depth scale, which is later than the end of the abrupt warming at 11,257 B.P. (1680.32 m) (Fig. 7). This observation suggests that the Greenland temperature rise preceded the atmospheric methane rise by at least 4 yr (0.20 m). However, atmospheric methane change is expected to lag climate change (methane emission change) by 5–10 yr owing to the atmospheric reservoir effect (Kobashi et al., 2007). Therefore, the climate change or methane emission change over a broad area could have been synchronous, as observed during the abrupt climate change at 8,200 year B.P. (Kobashi et al., 2007). We cannot exclude the possibility that the methane emission change actually lagged the Greenland temperature change by several decades. A higher resolution methane record will shed light on this issue.

4.2. Causes of abrupt climate changes

4.2.1. Ocean circulation modes

The cause of the Preboreal Oscillation cooling has been hypothesized to be melt water input (maximum 21,000 km^3 for 1.5–3 year) to the Arctic Ocean caused by a flood at ~11,335 B.P. from Lake Agassiz (Fisher et al., 2002). The fresher surface seawater might have enabled expanded winter sea ice cover, and the low salinity water may have impeded deepwater formation in the North Atlantic (Hald and Hagen, 1998; Meissner and Clark, 2006). The large fresh-water input into the North Atlantic may have driven the location of ocean ventilation toward the south, and may have reduced the strength of the meridional overturning circulation, leading to a reduced

heat and salt transport, thus enabling winter sea ice cover and cooling of Greenland mean-annual temperature (Ganopolski and Rahmstorf, 2001).

As no external forcing can explain the large abrupt warming events, which are often observed in the last glacial period, the cause has to lie in the internal dynamics of the ocean itself. It has been suggested that the ocean circulation in the Atlantic has two stable modes (Ganopolski and Rahmstorf, 2001; Rahmstorf, 2002). During the glacial period, the ocean is stable in the colder circulation mode, and only marginally stable in the warmer circulation mode. It has been shown that a switch from the colder to warmer mode can be easily triggered by a small forcing (Ganopolski and Rahmstorf, 2001), and the warming is greatly enhanced by a positive feedback in which low-latitude salty water is drawn into the sinking regions by the rejuvenated circulation, further enhancing the sinking (the so-called "advective feedback") (Ganopolski and Rahmstorf, 2001). This mechanism represents the leading hypothesis to explain the abrupt warmings (Ganopolski and Rahmstorf, 2001). We speculate that the oceanic condition after the termination of the Younger Dryas was still favorable to the colder circulation mode so that the ocean circulation gradually returned to the colder mode, possibly aided by fresh-water input. Then, a large abrupt warming was triggered by a small forcing such as changes in precipitation at 11,270 B.P. After the abrupt warming, the overall oceanic condition may have passed a threshold, and locked into the warm stable Holocene mode. The ^{14}C from tree-ring records have been used to link the climate change with the ocean overturning circulation or changes in solar activity (Fig. 1) (Bjorck et al., 1996; Bjorck et al., 1997; Bond et al., 2001; van Geel et al., 2003; Van der Plicht et al., 2004). However, our precise chronology does not show these previously claimed relationships (Fig. 1).

4.2.2. Similarities with Heinrich and Dansgaard–Oeschger events

The $\delta^{15}N$ record (Fig. 1) shows that there are four detectable peaks (numbered 1–4), which start with the abrupt warming event at the Younger Dryas termination. These peaks become successively smaller with time, as in a ringing oscillation. A broadly similar character is found during the last glacial period. A larger, longer-duration Dansgaard–Oeschger warm event seemingly follows a Heinrich event, and subsequent events become progressively smaller and shorter (Bond and Lotti, 1995; Huber et al., 2006b). The latest Heinrich-like event (H0) is found during the Younger Dryas (Bond and Lotti, 1995). This may suggest that the large abrupt warming events at the terminations of the Younger Dryas and Preboreal Oscillation, and the two smaller abrupt warmings (Fig. 1) might be a smaller manifestation of similar underlying physics as the Dansgaard–Oeschger events, in the Holocene, as suggested by Bond et al. (1997).

4.2.3. Comparison with the 8.2 ka event

About three thousand years after the Preboreal Oscillation and the subsequent abrupt warming event, the Holocene was punctuated by another large climate change at 8,200 yr B.P. (the 8.2 ka event) (Alley et al., 1997a; Kobashi et al., 2007). The 8.2 ka event had a similar magnitude of cooling and geographical extent as the Preboreal Oscillation (Kobashi et al., 2007). The 8.2 ka event is thought to have been caused by the largest outburst of a proglacial lake in the last 100,000 yr (Barber et al., 1999; Clarke et al., 2003). Temperature dropped by 3.3 ± 1.1 °C abruptly, and then temperature gradually rose to the condition prior to the event (Kobashi et al., 2007). The difference in temperature evolution between the Preboreal Oscillation and the 8.2 ka event suggests that two events are likely caused by different mechanisms. As discussed previously, the character of the Preboreal Oscillation is more similar to the Dansgaard–Oeschger events in the last glacial. On the other hand, at the time of the 8.2 ka event the ocean circulation may have already established a much more stable and warmer mode, which was only capable of being perturbed by a huge proglacial-lake outburst. Then, the ocean circulation gradually returned to the original state, without Dansgaard-Oeschger-like behavior.

5. Conclusion

We have shown that the hemispheric-scale climatic event, "the Preboreal Oscillation", was terminated with a rather abrupt warming of 4 ± 1.5 °C. Snow accumulation rate rose by 30% within a few years, suggesting a rapid reorganization of climate. The $\delta^{15}N$ record shows two large peaks over the interval 11,800 B.P. to 10,700 B.P. with two smaller subsequent peaks. We speculate that these "ringing" oscillations may be a smaller manifestation of the Dansgaard–Oeschger events, which characterized the cold unstable glacial ocean. The last large abrupt warming at 11,270 B.P. likely marks the onset of a warm and stable oceanic condition in the Holocene.

Acknowledgements

We appreciate thorough reviews by A. Landais and an anonymous reviewer. We thank R.A. Beaudette and the National Ice Core Laboratory (NICL) for ice sample assistance, and K. Kawamura for discussion. We acknowledge T. Crowley and E. Brook for helpful comments on the earlier manuscript. We thank Michael Friedrich and Raimund Muscheler for sharing the information on the chronology. Data are available upon request to the authors (T. K. or J.P.S.). This work was supported by NSF grants OPP 05-38657 and ATM 99-05241 (to J.P.S.).

Appendix A. Supplementary data

Supplementary data associated with this article can be found, in the online version, at doi:10.1016/j.epsl.2008.01.032.

References

Allegre, C.J., Staudacher, T., Sarda, P., 1987. Rare-Gas Systematics — Formation of the Atmosphere, Evolution and Structure of the Earths Mantle. Earth Planet. Sci. Lett. 81, 127–150.

Alley, R.B., Mayewski, P.A., Sowers, T., Stuiver, M., Taylor, K.C., Clark, P.U., 1997a. Holocene climatic instability: A prominent, widespread event 8200 yr ago. Geology 25, 483–486.

Alley, R.B., Meese, D.A., Shuman, C.A., Gow, A.J., Taylor, K.C., Grootes, P.M., White, J.W.C., Ram, M., Waddington, E.D., Mayewski, P.A., Zielinski, G.A., 1993. Abrupt Increase in Greenland Snow Accumulation at the End of the Younger Dryas Event. Nature 362, 527–529.

Alley, R.B., Shuman, C.A., Meese, D.A., Gow, A.J., Taylor, K.C., Cuffey, K.M., Fitzpatrick, J.J., Grootes, P.M., Zielinski, G.A., Ram, M., Spinelli, G., Elder, B., 1997b. Visual-stratigraphic dating of the GISP2 ice core: Basis, reproducibility, and application. J. Geophys. Res. Oceans 102, 26367–26381.

Barber, D.C., Dyke, A., Hillaire-Marcel, C., Jennings, A.E., Andrews, J.T., Kerwin, M.W., Bilodeau, G., McNeely, R., Southon, J., Morehead, M.D., Gagnon, J.M., 1999. Forcing of the cold event of 8,200 years ago by catastrophic drainage of Laurentide lakes. Nature 400, 344–348.

Bard, E., Hamelin, B., Arnold, M., Montaggioni, L., Cabioch, G., Faure, G., Rougerie, F., 1996. Deglacial sea-level record from Tahiti corals and the timing of global meltwater discharge. Nature 382, 241–244.

Bender, M., Sowers, T., Lipenkov, V., 1995. On the Concentrations of O-2, N-2, and Ar in Trapped Gases from Ice Cores. J. Geophys. Res. Atmospheres 100, 18651–18660.

Bjorck, S., Kromer, B., Johnsen, S., Bennike, O., Hammarlund, D., Lemdahl, G., Possnert, G., Rasmussen, T.L., Wohlfarth, B., Hammer, C.U., Spurk, M., 1996. Synchronized terrestrial-atmospheric deglacial records around the North Atlantic. Science 274, 1155–1160.

Bjorck, S., Rundgren, M., Ingolfsson, O., Funder, S., 1997. The Preboreal oscillation around the Nordic Seas: terrestrial and lacustrine responses. J. Quat. Sci. 12, 455–465.

Bond, G., Kromer, B., Beer, J., Muscheler, R., Evans, M.N., Showers, W., Hoffmann, S., Lotti-Bond, R., Hajdas, I., Bonani, G., 2001. Persistent solar influence on north Atlantic climate during the Holocene. Science 294, 2130–2136.

Bond, G., Showers, W., Cheseby, M., Lotti, R., Almasi, P., deMenocal, P., Priore, P., Cullen, H., Hajdas, I., Bonani, G., 1997. A pervasive millennial-scale cycle in North Atlantic Holocene and glacial climates. Science 278, 1257–1266.

Bond, G.C., Lotti, R., 1995. Iceberg Discharges into the North-Atlantic on Millennial Time Scales During the Last Glaciation. Science 267, 1005–1010.

Brook, E.J., Harder, S., Severinghaus, J., Steig, E.J., Sucher, C.M., 2000. On the origin and timing of rapid changes in atmospheric methane during the last glacial period. Glob. Biogeochem. Cycles 14, 559–572.

Charles, C.D., Rind, D., Jouzel, J., Koster, R.D., Fairbanks, R.G., 1994. Glacial–Interglacial Changes in Moisture Sources for Greenland — Influences on the Ice Core Record of Climate. Science 263, 508–511.

Clarke, G., Leverington, D., Teller, J., Dyke, A., 2003. Superlakes, megafloods, and abrupt climate change. Science 301, 922–923.

Colbeck, S.C., 1989. Air Movement in Snow Due to Windpumping. J. Glaciol. 35, 209–213.

Craig, H., Horibe, Y., Sowers, T., 1988. Gravitational Separation of Gases and Isotopes in Polar Ice Caps. Science 242, 1675–1678.

Cuffey, K.M., Clow, G.D., 1997. Temperature, accumulation, and ice sheet elevation in central Greenland through the last deglacial transition. J. Geophys. Res. Oceans 102, 26383–26396.

Cuffey, K.M., Clow, G.D., Alley, R.B., Stuiver, M., Waddington, E.D., Saltus, R.W., 1995. Large Arctic Temperature-Change at the Wisconsin–Holocene Glacial Transition. Science 270, 455–458.

Fairbanks, R.G., 1989. A 17,000-Year Glacio-Eustatic Sea-Level Record — Influence of Glacial Melting Rates on the Younger Dryas Event and Deep-Ocean Circulation. Nature 342, 637–642.

Finkel, R.C., Nishiizumi, K., 1997. Beryllium 10 concentrations in the Greenland Ice Sheet Project 2 ice core from 3–40 ka. J. Geophys. Res. Oceans 102, 26699–26706.

Fisher, T.G., Smith, D.G., Andrews, J.T., 2002. Preboreal oscillation caused by a glacial Lake Agassiz flood. Quat. Sci. Rev. 21, 873–878.

Friedrich, M., Kromer, B., Spurk, H., Hofmann, J., Kaiser, K.F., 1999. Paleo-environment and radiocarbon calibration as derived from Lateglacial/Early Holocene tree-ring chronologies. Quat. Int. 61, 27–39.

Friedrich, M., Remmelel, S., Kromer, B., Hofmann, J., Spurk, M., Kaiser, K.F., Orcel, C., Kuppers, M., 2004. The 12,460-year Hohenheim oak and pine tree-ring chronology from central Europe — A unique annual record for radiocarbon calibration and paleoenvironment reconstructions. Radiocarbon 46, 1111–1122.

Ganopolski, A., Rahmstorf, S., 2001. Rapid changes of glacial climate simulated in a coupled climate model. Nature 409, 153–158.

Goujon, C., Barnola, J.M., Ritz, C., 2003. Modeling the densification of polar firn including heat diffusion: Application to close-off characteristics and gas isotopic fractionation for Antarctica and Greenland sites. J. Geophys. Res. Atmospheres 108.

Grachev, A.M., 2004. Laboratory-determined air thermal diffusion constants applied to reconstructing the magnitudes of past abrupt temperature changes from gas isotope observations in polar ice cores. Dissertation.

Grachev, A.M., Severinghaus, J.P., 2003a. Determining the thermal diffusion factor for Ar-40/Ar-36 in air to aid paleoreconstruction of abrupt climate change. J. Phys. Chem. A 107, 4636–4642.

Grachev, A.M., Severinghaus, J.P., 2003b. Laboratory determination of thermal diffusion constants for N-29(2)/N-28(2) in air at temperatures from−60 to 0 degrees C for reconstruction of magnitudes of abrupt climate changes using the ice core fossil–air paleothermometer. Geochim. Cosmochim. Acta 67, 345–360.

Grachev, A.M., Severinghaus, J.P., 2005. A revised +10 +/−4 degrees C magnitude of the abrupt change in Greenland temperature at the Younger Dryas termination using published GISP2 gas isotope data and air thermal diffusion constants. Quat. Sci. Rev. 24, 513–519.

Hald, M., Hagen, S., 1998. Early preboreal cooling in the Nordic seas region triggered by meltwater. Geology 26, 615–618.

Hu, F.S., Nelson, D.M., Clarke, G.H., Ruhland, K.M., Huang, Y.S., Kaufman, D.S., Smol, J.P., 2006. Abrupt climatic events during the last glacial–interglacial transition in Alaska. Geophys. Res. Lett. 33.

Huber, C., Beyerle, U., Leuenberger, M., Schwander, J., Kipfer, R., Spahni, R., Severinghaus, J.P., Weiler, K., 2006a. Evidence for molecular size dependent gas fractionation in firn air derived from noble gases, oxygen, and nitrogen measurements. Earth Planet. Sci. Lett. 243, 61–73.

Huber, C., Leuenberger, M., Spahni, R., Fluckiger, J., Schwander, J., Stocker, T.F., Johnsen, S., Landals, A., Jouzel, J., 2006b. Isotope calibrated Greenland temperature record over Marine Isotope Stage 3 and its relation to CH4. Earth Planet. Sci. Lett. 243, 504–519.

Hughen, K.A., Overpeck, J.T., Peterson, L.C., Trumbore, S., 1996. Rapid climate changes in the tropical Atlantic region during the last deglaciation. Nature 380, 51–54.

Jouzel, J., Alley, R.B., Cuffey, K.M., Dansgaard, W., Grootes, P., Hoffmann, G., Johnsen, S.J., Koster, R.D., Peel, D., Shuman, C.A., Stievenard, M., Stuiver, M., White, J., 1997. Validity of the temperature reconstruction from water isotopes in ice cores. J. Geophys. Res. Oceans 102, 26471–26487.

Kawamura, K., Severinghaus, J.P., Ishidoya, S., Sugawara, S., Hashida, G., Motoyama, H., Fujii, Y., Aoki, S., Nakazawa, T., 2006. Convective mixing of air in firn at four polar sites. Earth Planet. Sci. Lett. 244, 672–682.

Kobashi, T., 2007. Greenland temperature, climate change, and human society during the last 11,600 years. Ph.D. thesis, University of California, San Diego.

Kobashi, T., Severinghaus, J., Brook, E.J., Barnola, J.M., Grachev, A., 2007. Precise timing and characterization of abrupt climate change 8,200 years ago from air trapped in polar ice. Quat. Sci. Rev. doi:10.1016/j-quascirev.2007.01.009.

Landais, A., Barnola, J.M., Masson-Delmotte, V., Jouzel, J., Chappellaz, J., Caillon, N., Huber, C., Leuenberger, M., Johnsen, S.J., 2004a. A continuous record of temperature evolution over a sequence of Dansgaard–Oeschger events during Marine Isotopic Stage 4 (76 to 62 kyr BP). Geophys. Res. Lett. 31.

Landais, A., Caillon, N., Goujon, C., Grachev, A.M., Barnola, J.M., Chappellaz, J., Jouzel, J., Masson-Delmotte, V., Leuenberger, M., 2004b. Quantification of rapid temperature change during DO event 12 and phasing with methane inferred from air isotopic measurements. Earth Planet. Sci. Lett. 225, 221–232.

Lang, C., Leuenberger, M., Schwander, J., Johnsen, S., 1999. 16 degrees C rapid temperature variation in Central Greenland 70,000 years ago. Science 286, 934–937.

Leuenberger, M.C., Lang, C., Schwander, J., 1999. Delta(15)N measurements as a calibration tool for the paleothermometer and gas-ice age differences: A case study for the 8200 BP event on GRIP ice. J. Geophys. Res. Atmospheres 104, 22163–22170.

Li, J., Zwally, H.J., Cornejo, C., Yi, D.H., 2003. Seasonal variation of snow-surface elevation in North Greenland as modeled and detected by satellite radar altimetry. Ann. Glaciol. 37, 233–238.

Mariotti, A., 1983. Atmospheric Nitrogen Is a Reliable Standard for Natural N-15 Abundance Measurements. Nature 303, 685–687.

Meissner, K.J., Clark, P.U., 2006. Impact of floods versus routing events on the thermohaline circulation. Geophys. Res. Lett. 33.

Rahmstorf, S., 2002. Ocean circulation and climate during the past 120,000 years. Nature 419, 207–214.

Reimer, P.J., Baillie, M.G.L., Bard, E., Bayliss, A., Beck, J.W., Bertrand, C.J.H., Blackwell, P.G., Buck, C.E., Burr, G.S., Cutler, K.B., Damon, P.E., Edwards, R.L., Fairbanks, R.G., Friedrich, M., Guilderson, T.P., Hogg, A.G., Hughen, K.A., Kromer, B., McCormac, G., Manning, S., Ramsey, C.B., Reimer, R.W., Remmele, S., Southon, J.R., Stuiver, M., Talamo, S., Taylor, F.W., van der Plicht, J., Weyhenmeyer, C.E., 2004. IntCal04 terrestrial radiocarbon age calibration, 0–26 cal kyr BP. Radiocarbon 46, 1029–1058.

Schwander, J., Barnola, J.M., Andrie, C., Leuenberger, M., Ludin, A., Raynaud, D., Stauffer, B., 1993. The Age of the Air in the Firn and the Ice at Summit, Greenland. J. Geophys. Res. Atmospheres 98, 2831–2838.

Schwander, J., Sowers, T., Barnola, J.M., Blunier, T., Fuchs, A., Malaize, B., 1997. Age scale of the air in the summit ice: Implication for glacial–interglacial temperature change. J. Geophys. Res. Atmospheres 102, 19483–19493.

Seppa, H., Birks, H.H., Birks, H.J.B., 2002. Rapid climatic changes during the Greenland stadial 1 (Younger Dryas) to early Holocene transition on the Norwegian Barents Sea coast. Boreas 31, 215–225.

Severinghaus, J.P., Battle, M.O., 2006. Fractionation of gases in polar lee during bubble close-off: New constraints from firn air Ne, Kr and Xe observations. Earth Planet. Sci. Lett. 244, 474–500.

Severinghaus, J.P., Brook, E.J., 1999. Abrupt climate change at the end of the last glacial period inferred from trapped air in polar ice. Science 286, 930–934.

Severinghaus, J.P., Grachev, A., Battle, M., 2001. Thermal fractionation of air in polar firn by seasonal temperature gradients. Geochem. Geophys. Geosyst. 2 art. no.-2000GC000146.

Severinghaus, J.P., Grachev, A., Luz, B., Caillon, N., 2003. A method for precise measurement of argon 40/36 and krypton/argon ratios in trapped air in polar ice with applications to past firn thickness and abrupt climate change in Greenland and at Siple Dome, Antarctica. Geochim. Cosmochim. Acta 67, 325–343.

Severinghaus, J.P., Sowers, T., Brook, E.J., Alley, R.B., Bender, M.L., 1998. Timing of abrupt climate change at the end of the Younger Dryas interval from thermally fractionated gases in polar ice. Nature 391, 141–146.

Sowers, T., Bender, M., Raynaud, D., Korotkevich, Y.S., 1992. Delta-N-15 of N2 in Air Trapped in Polar Ice — a Tracer of Gas-Transport in the Firn and a Possible Constraint on Ice Age–Gas Age-Differences. J. Geophys. Res. Atmospheres 97, 15683–15697.

Stuiver, M., Grootes, P.M., Braziunas, T.F., 1995. The GISP2 delta O-18 climate record of the past 16,500 years and the role of the sun, ocean, and volcanoes. Quat. Res. 44, 341–354.

Van der Plicht, J., Van Geel, B., Bohncke, S.J.P., Bos, J.A.A., Blaauw, M., Speranza, A.O.M., Muscheler, R., Bjorck, S., 2004. The Preboreal climate reversal and a subsequent solar-forced climate shift. J. Quat. Sci. 19, 263–269.

van Geel, B., van der Plicht, J., Renssen, H., 2003. Major Delta C-14 excursions during the late glacial and early Holocene: changes in ocean ventilation or solar forcing of climate change? Quat. Int. 105, 71–76.

Vinther, B.M., Clausen, H.B., Johnsen, S.J., Rasmussen, S.O., Andersen, K.K., Buchardt, S.L., Dahl-Jensen, D., Seierstad, I.K., Siggaard-Andersen, M.L., Steffensen, J.P., Svensson, A., Olsen, J., Heinemeier, J., 2006. A synchronized dating of three Greenland ice cores throughout the Holocene. J. Geophys. Res. Atmospheres 111.

White, J.W.C., Barlow, L.K., Fisher, D., Grootes, P., Jouzel, J., Johnsen, S.J., Stuiver, M., Clausen, H., 1997. The climate signal in the stable isotopes of snow from Summit, Greenland: Results of comparisons with modern climate observations. J. Geophys. Res. Oceans 102, 26425–26439.

Yu, Z.C., Eicher, U., 1998. Abrupt climate oscillations during the last deglaciation in central North America. Science 282, 2235–2238.

Zwally, H.J., Jun, L., 2002. Seasonal and interannual variations of firn densification and ice-sheet surface elevation at the Greenland summit. J. Glaciol. 48, 199–207.